NACA TN 3821

NATIONAL ADVISORY COMMITTEE FOR AERONAUTICS

TECHNICAL NOTE 3821

FLIGHT TECHNIQUES FOR DETERMINING AIRPLANE DRAG AT HIGH MACH NUMBERS

By De E. Beeler, Donald R. Bellman, and Edwin J. Saltzman

NACA High-Speed Flight Station
Edwards, Calif.

Washington

August 1956

NATIONAL ADVISORY COMMITTEE FOR AERONAUTICS

TECHNICAL NOTE 3821

FLIGHT TECHNIQUES FOR DETERMINING AIRPLANE DRAG AT HIGH MACH NUMBERS[1]

By De E. Beeler, Donald R. Bellman, and Edwin J. Saltzman

SUMMARY

The measurement of total airplane drag in flight is necessary to assess the applicability of wind-tunnel model data. The NACA High-Speed Flight Station has investigated and developed techniques for measuring the drag of high-speed research airplanes and current fighter-type airplanes. The accelerometer method for determining drag was found to be the most satisfactory method for research work, because it is the only method permitting a complete coverage of the Mach number and angle-of-attack capabilities of an airplane.

Determining drag by the accelerometer method requires the accurate measurement of longitudinal and normal accelerations, angle of attack, and engine thrust. In addition, the static pressure, airspeed, airplane weight, and longitudinal control positions must be measured. The accurate measurement of longitudinal and normal acceleration can be made and recorded by means of specially constructed mechanical accelerometers that have been developed by the NACA. Fuselage nose booms are used to reduce the flow-field errors in the measurement of static pressure, airspeed, and angle of attack. The errors can be reduced further to an acceptable level by established calibration techniques. Satisfactory methods for determining in flight the thrust of turbojet-afterburner and rocket engines are available.

The flight drag data generally can be separated into components consisting of trim, skin-friction, pressure-induced, and wave drags. The comparison of flight and wind-tunnel data must be made on the basis of component drags if a proper interpretation of the results is to be obtained.

INTRODUCTION

Considerable research effort has been directed in recent years toward improving the performance of aircraft to achieve efficient supersonic flight. The verification and evaluation of the latest thinking, for the

[1]This report was presented to the Flight Test Panel of the NATO Advisory Group for Aeronautical Research and Development at the meeting in Brussels, Belgium, August 27-31, 1956.

most part, is a result of model testing. However, questions on the adequacy of the model tests are raised when effects of scale and power are considered. It is necessary, therefore, that selected full-scale flight investigations of the airplane drag be made to assess the value of calculations based on model information. The value of the flight investigations of airplane drag is, of course, dependent on the accuracies with which the flight data may be measured. Investigations of the drag characteristics of research-type aircraft have been conducted at the NACA High-Speed Flight Station since the inception of the NACA-Military Services-Industry Research Airplane Program. More recently, the techniques and methods developed and used for these aircraft have been extended to the latest high-performance service aircraft.

This paper describes the flight techniques used to determine the total airplane drag including the effects of thrust. Some consideration is given to the use of flight data for comparison with wind-tunnel results.

SYMBOLS

A	cross-sectional area of exhaust jet stream, sq ft
A_d	cross-sectional area of inlet duct, sq ft
A_e	rocket-nozzle exit area, sq ft
A_L	measured airplane longitudinal acceleration, g units
A_t	rocket-nozzle throat area, sq ft
A_X	true airplane longitudinal acceleration, g units
A_Z	true airplane normal acceleration, g units
a_d	velocity of sound in inlet duct, ft/sec
a_0	velocity of sound under ambient conditions, ft/sec
C_D	drag coefficient, D/qS
C_{D_f}	friction drag coefficient
C_{D_p}	parasite drag coefficient
C_f	jet-nozzle coefficient
C_L	lift coefficient, L/qS

C_N	normal-force coefficient, nW/qS
C_X	axial-force coefficient, D_X/qS
c,c'	constants
D	drag force along airplane flight path, lb
D_X	drag force along airplane axis, lb
D_{max}	maximum equivalent fuselage diameter, ft
E_A	total airplane energy, ft-lb
F_j	engine jet thrust, lb
F_n	engine net thrust, lb
F_r	ram drag of inlet air, lb
g	acceleration of gravity, ft/sec^2
h	altitude, ft
L	airplane lift normal to flight path, lb
L_N	airplane lift normal to airplane axis, lb
M	airplane Mach number
M_d	Mach number within inlet duct
N	engine speed, rpm
n	normal-load factor, g units
P	total pressure, lb/sq ft
p	static pressure, lb/sq ft
p_c	rocket combustion-chamber pressure, lb/sq ft
p_d	static pressure in inlet duct, lb/sq ft
p_e	rocket-nozzle exit static pressure, lb/sq ft
p_0	ambient pressure, lb/sq ft
q	dynamic pressure, lb/sq ft

R	gas constant, ft/^{o}R
R	Reynolds number
r_b	radius of nose boom
r_v	distance from nose boom center line to center of flow-indicating vane
S	wing area, sq ft
T	static temperature, ^{o}R
T_d	static temperature in inlet duct, ^{o}R
T_t	total temperature, ^{o}R
T_0	ambient temperature, ^{o}R
t	time, sec
V	velocity, ft/sec
V_d	air velocity in inlet duct, ft/sec
V_0	airplane velocity, ft/sec
W	airplane weight, lb
w	mass-flow rate, lb-sec/ft
w_a	air mass-flow rate, lb-sec/ft
w_f	fuel mass-flow rate, lb-sec/ft
X	distance from static-pressure orifices to fuselage nose, ft
X'	distance from flow-direction vane to fuselage nose, ft
α	airplane angle of attack (angle between airplane axis and flight path), deg
α_i	indicated angle of attack, deg
α_t	true angle of attack, deg
γ	flight-path angle (angle between flight path and the horizontal), deg

γ ratio of specific heats of gases

$\Delta\alpha$ error in angle of attack, deg

ΔM error in Mach number

Δt time increment, sec

δ altitude normalizing factor, $P/2116$

θ temperature normalizing factor, $T_t/518.4$

ρ gas density, lb/cu ft

ρ_d density of air in inlet duct, lb/cu ft

ρ_0 atmospheric density, lb/cu ft

METHODS

The method used for determining airplane drag from flight data depends on the degree to which desired flight conditions can be attained, the accuracy and extent of instrumentation in the airplane, the facilities available for reducing the data, and the coverage in angle of attack and Mach number desired in the investigation. Several methods have been suggested and used previously, as presented in references 1 to 4. The methods considered by the NACA High-Speed Flight Station as applicable to supersonic aircraft have been the stabilized flight, energy, and accelerometer methods. These methods are discussed in the following sections.

Stabilized Flight Method

The stabilized flight method is by far the simplest of the three methods for determining airplane drag. The method consists merely of a constant-altitude, fixed-throttle flight of sufficient duration to enable the airplane to reach a stabilized speed. Under these conditions it is assumed that the drag is equal to the thrust.

One disadvantage of this method is that truly stabilized flight, which is essential for accurate application of the method, is seldom achieved and, even if achieved, is difficult to ascertain. This is particularly true at high Mach numbers and at flight conditions where the aircraft stability is marginal.

This method has the additional disadvantages of not allowing coverage of the entire angle-of-attack and Mach number ranges of which the airplane is capable, and of requiring a large amount of flight time to obtain a given amount of data. For a given speed the angle-of-attack variations can be obtained only by varying the airplane weight and altitude; consequently, the obtainable angle-of-attack range is limited. Some investigators average the data from a wide range of altitude and Mach number below the drag-rise Mach number in order to construct a single drag polar. This procedure obscures any effects of Mach number and altitude. In addition to obtaining only a single data point at a given Mach number and altitude, the time required to reach stabilized conditions, particularly at high speed, greatly reduces the amount of data that can be obtained during any one flight.

It is concluded that the stabilized flight method is basically unsatisfactory for flight research but might be suitable for routine checking of production airplanes.

Energy Method

The energy method sums up, over an incremental time period, the energy changes involved in engine thrust, altitude variations, and flight speed variations. It is essentially an extension of the stabilized flight method and allows some variations in speed and altitude. The method permits data to be obtained in the high-speed dives needed to approach the maximum speed capabilities of an airplane.

The disadvantages of this method are similar to those previously noted for the stabilized flight method. In addition, use of the incremental time period requires extremely high accuracy in measuring altitude and velocity if excessively long time increments are to be avoided. The use of long time increments may result in averaging the data over angle-of-attack increments that are too large for acceptable accuracy.

Accelerometer Method

The accelerometer method permits integration of all aerodynamic, gravitational, momentum, and inertia forces on an airplane at any given instant regardless of airplane attitude or acceleration. Thus, the only unknown major component will be the total airplane drag. This method is readily applicable to gradual maneuvering flight and permits a complete coverage of angle-of-attack and Mach number range in a minimum number of flights. Application of this method requires the use of very sensitive longitudinal accelerometers and an accurate means of measuring angle of attack, in addition to the more customary research instruments.

The NACA has developed and flight-tested sensitive instruments by means of which the accelerometer method can be adequately applied to the flight determination of drag. By using these instruments, the method has been employed to determine the drag characteristics of the research-type and high-performance service aircraft flown at the NACA High-Speed Flight Station. Further discussion of the flight measurements required to measure airplane drag will therefore be pertinent to the use of the accelerometer method.

The advantage of the accelerometer method over the energy method for the determination of drag during a maneuver is presented graphically in figure 1. The figure shows the drag polars obtained by the energy method for time increments of 1, 2, and 4 seconds, and by the accelerometer method. The data are from a typical push-down, pull-up maneuver covering a total time of 24 seconds. The derivation and description of the equations used with the accelerometer and energy methods are presented in appendix A.

MEASUREMENTS

The determination of total airplane drag by means of the accelerometer method requires the continuous measurement and recording of many quantities during each flight maneuver. Certain of these measurements such as longitudinal and normal acceleration, angle of attack, and engine thrust require the highest degree of instrument accuracy and measurement technique in order to avoid excessive error in the drag data. These measurements are discussed in detail in the following sections. Other measurements such as static pressure which is needed for the determination of altitude and Mach number, airplane weight, and control positions have less effect on the accuracy of the drag data but are discussed because of the various techniques that can be employed. In addition, the measurement of pitching velocity is needed to make corrections to the angle-of-attack measurements.

Acceleration

At the NACA High-Speed Flight Station the precise measurement of the longitudinal acceleration of research airplanes is obtained with an NACA developed accelerometer of the type shown schematically in figure 2. The accelerometer is magnetically damped and operates on a mechanical-optical principle as follows: The inertial mass consists of a pivoted aluminum vane between the poles of a permanent magnet. Attached to the shaft is a mirror which reflects a beam of light to a moving strip of photographic film. The beam of light will then be deflected in proportion

to the vane movement which is restrained by springs. The damping, which can be adjusted by varying the gap between the poles, is generally set at about 65 percent of critical damping. The natural frequency of the vanes varies with the range of the instruments. It is about 10 cycles per second for an instrument having a range of ±1g, and about 18 cycles per second for an instrument having a range of ±0.5g. The lower range instruments are suitable for most of the airplanes powered by turbojet engines; the higher range instruments are required for some of the rocket-propelled airplanes.

For measuring the longitudinal acceleration of an airplane, the instrument will be mounted so that the pivot axis of the vane will parallel the normal axis of the airplane, and so the line connecting the pivot axis of the vane with the center of mass of the vane, when in the neutral position, will be parallel to the lateral axis of the airplane. In this position the longitudinal-acceleration measurements will be unaffected by normal acceleration; the only possible carryover effect can result from transverse acceleration which has negligible effect for maneuvers of the type used for drag determination. The importance of possible carryover effects cannot be emphasized too strongly. Laboratory tests of one model of a strain-gage-type accelerometer showed appreciable carryover components from both the other axes. For example, carryover effects to the longitudinal acceleration by an amount of 5 percent of the normal acceleration have been found. This error for drag data measured at a normal acceleration of 5g would result in an error of 0.2g in longitudinal acceleration. The error in longitudinal acceleration could be equal to the value of the acceleration to be measured for drag.

If space limitations cause the accelerometer to be mounted a significant distance from the airplane center of gravity, corrections must be applied to eliminate the effects of pitching velocity and pitching acceleration. It should also be noted that the longitudinal accelerometer must be accurately alined with the airplane longitudinal axis to prevent an effect of the normal acceleration.

Normal accelerations of the airplane must also be measured, but not to so great an accuracy as longitudinal accelerations. The NACA uses a similar, but broader-range, instrument for this measurement.

Angle of Attack

Measurement of angle of attack in flight has been a source of considerable research because of the importance of the measurement in determining airplane drag, particularly for high-lift conditions. For the accelerometer method the error in drag caused by angle-of-attack error is equal to the product of the lift and the angle-of-attack error.

Various types of angle-of-attack sensing devices have been investigated by the NACA. It was found that the most accurate and reliable results could be obtained with a pivoted vane mounted on a nose boom as far ahead of the airplane as practicable. A typical example of a nose boom with angle-of-attack and angle-of-sideslip vanes is presented in figure 3. The vane is directly connected to a Selsyn motor within the boom which in turn electrically actuates a receiver motor within the airplane and moves a beam of light across a moving strip of film. While this system is capable of measuring the vane position within 0.1°, the flow angle registered by the vane does not necessarily represent the true angle of attack of the airplane because of the effects of pitching velocity, boom and fuselage bending, and upwash. Pitching velocity will introduce an air-velocity component across the flight path, thus providing an erroneous angle-of-attack indication. These errors may be evaluated from measurements of the airplane pitching velocity during the test maneuvers.

Bending of the boom from normal loads due to inertia and air loads will result in errors in the measured angle of attack because the deflections of the angle-of-attack vane are normally referenced to the axis of the support boom. Boom bending resulting from inertia loading can be corrected from results of a static deflection calibration of the boom loaded under a proper weight distribution. Bending of the boom resulting from aerodynamic loading may be corrected on a basis of calculated aerodynamic loading of the boom (ref. 5). For boom installations used at the NACA High-Speed Flight Station, the deflections due to aerodynamic loading are negligible. For special cases of extremely long booms, it has been suggested that the boom loading due to the combined inertia and aerodynamic loading be determined by photographing the boom deflection during flight. Fuselage bending corrections may be necessary for extremely long flexible fuselages and could be determined in the same manner as for the boom.

Upwash is one of the most troublesome problems involved in measuring angle of attack since it stems from the wing, the fuselage, and the boom. Upwash error caused by the boom itself can be measured by a wind-tunnel calibration of the system and corrections applied to the flight data. References 6 and 7 present calibration data on boom configurations used extensively by the NACA.

Two-dimensional incompressible-flow theory as presented in reference 8 can be used to compute some of the low-speed upwash effects. The theory indicates that the angle-of-attack error resulting from upwash because of the boom will be proportional to the square of the ratio of boom radius to the distance of the vane from the center of the boom. A plot of the effect is presented in figure 4. Also shown in figure 4 is the variation of angle-of-attack error, resulting from upwash around a blunt circular

fuselage, with distance ahead of the fuselage. The data for this curve were calculated by using the method presented in reference 9. The effect of upwash around the wing on the angle-of-attack measurements can be calculated by equations presented in reference 8 for unswept-wing airplanes and by methods presented in reference 10 for swept-wing airplanes. The effect on angle-of-attack measurements of upwash due to the wing is generally much less than that due to the fuselage and boom where the boom is mounted on the fuselage nose.

Attempts have been made to calibrate the angle-of-attack measuring system on an absolute basis in flight by measuring and recording the airplane attitude and flight path. However, airplane attitude is difficult to establish and requires a stable reference such as the horizon or the sun. Some exploratory work on such an angle-of-attack calibration has been done at the High-Speed Flight Station with the sun as an attitude reference. Results of an investigation conducted on the X-5 airplane are shown in figure 5. The data show the expected error in angle of attack with increasing angle of attack and the decrease in error with increasing Mach number. It should be pointed out that such calibrations are tedious and time consuming and that, for the purpose of determining drag at high subsonic or supersonic speeds and at moderate angles of attack, sufficiently accurate measurements of angle of attack can be made without recourse to such a calibration.

Thrust

The measurement of engine thrust is one of the more difficult problems in determining total airplane drag. With the advent of jet airplanes and the large increases in thrust-to-weight ratios, the measurement of thrust has become increasingly important. Fortunately, the definition and determination of thrust is somewhat simpler for turbojet and rocket airplanes than for propeller airplanes. The commonly accepted definition of jet and rocket engine thrust is the force caused by the change in momentum of the fluids passing through the engine system plus any unbalanced static stream pressures in the case of sonic or supersonic flows.

Turbojet engines (including afterburners).- The thrust of a turbojet engine is generally determined by means of pressure-sensing probes located at strategic points in the duct system. The thrust measurement is usually accomplished in two steps. First the exit momentum, referred to as the jet or gross thrust, is determined; then the inlet momentum, termed the ram drag, is determined and subtracted from the jet thrust to give the net thrust.

The equations for calculating the jet thrust from the various pressure and temperature measurements are derived in appendix B. The basic thrust equation is equation (B10) of appendix B. It will be noted that

the jet thrust can be determined by means of the measurement of only total and static pressure at the tailpipe exit. Total-pressure surveys are generally easier to make and are more accurate than static-pressure surveys; frequently assumptions are made to eliminate the need for static-pressure measurements in the jet exhaust. These assumptions result in different equations for subsonic and sonic flows, as given by equations (B11) and (B12) of appendix B, respectively. The ratio of specific heats of the gases γ varies with temperature, but the variation has a relatively minor effect on the thrust so that constant values of 1.40, 1.33, and 1.25 can be assumed for air, turbine outlet gas, and afterburner outlet gas, respectively.

One problem in measuring the tailpipe total pressure is that of obtaining a reasonable average across the tailpipe area without using an excessive number of probes, which create cooling problems in afterburner engines and losses in thrust. For some engines a single pitot probe extending into the exhaust-gas stream has proved adequate. Figure 6 shows a single, air-cooled, fixed pitot probe located at the tailpipe exit on a turbojet-afterburner combination. For other engines, swinging probes which periodically traverse the tailpipe exit proved successful. Figure 7 shows such an installation, and reference 11 gives details and results of a similar installation. The traverses of the swinging probe generally cover a period of 4 or 5 seconds and sufficient time is spent outside the hot-gas stream so that no cooling is required. Another type of installation that has been used particularly as a calibration means is a rake, with a large number of probes, which extends completely across the tailpipe. Reference 12 gives details on such an installation.

Because of the compromises necessary in the installation of the probes, certain errors exist in the thrust measurements. These errors can be reduced to a large extent by calibrating the probe installation, which necessitates placing the airplane on a thrust stand. The ratio of the probe-measured thrust to the true thrust is known as the nozzle coefficient C_f and is generally plotted against the ratio of tailpipe total pressure to ambient pressure. A typical example of such a plot is shown in figure 8, which is for a single-point air-cooled probe similar to the probe shown in figure 6. It will be noted that the calibration curves are extrapolated considerably beyond the ground-calibration data because exhaust pressure ratios will be encountered in flight that are two or three times the maximum obtainable on the ground. The extrapolation is not entirely arbitrary, however, because altitude-chamber tests of engines indicate that the curves round off and that there is little change above pressure ratios of about 2.2.

The use of a single pitot probe in conjunction with a ground calibration for determining jet thrust assumes that the general shape of the total-pressure profile across the tailpipe will not vary with Mach number and altitude. Preliminary tests with a swinging tailpipe probe at the

High-Speed Flight Station have shown no significant profile variations for a current production engine for altitudes up to 40,000 feet. However, reference 12 shows a slight variation and unpublished data on another engine indicate a large variation in profile with altitude. Consequently, the applicability of the single-pitot method will depend on the specific engine being used.

The assumptions concerning the static pressure at the tailpipe exit are somewhat open to question, and there is evidence that the static pressure is not exactly that assumed (ref. 12). If the static pressure could be measured along with total pressure on a swinging rake, for example, then the jet thrust could be computed from equation (B10) of appendix B. However, the tailpipe velocities are generally very close to sonic velocity and static-pressure measurements under such conditions are subject to extreme error, as indicated in references 11, 13, and 14.

As turbojet engines become more complicated, additional problems arise in the measurement of jet thrust. For example, some engines have cooling air flows of sufficient quantity and velocity that they must be considered. Other engines use an ejector which makes the exit area needed for use in the thrust equations a variable and uncertain quantity. In these instances, the swinging probe is proving to be of considerable advantage.

The ram drag of a turbojet engine is generally measured by one of three methods as given in appendix B. The tailpipe-temperature method is probably the least accurate because of the difficulty in measuring the hot-gas temperature. Reference 11 shows the enormous errors caused by lag when temperature measurements are made with a swinging probe. The use of the engine compressor air-flow curves is probably the most common method employed today and has proved quite satisfactory. This method depends on the standardization of engines, because separate compressor flow curves are generally not available for each individual engine but only for the various series of each type. The method requires the measurement of total temperature and total pressure at the compressor face. However, total temperature changes so little within the duct that a single reading of total temperature somewhere on the forward part of the airplane generally suffices both for the compressor air-flow measurement and for obtaining airplane velocity from airplane Mach number as indicated by equation (B15) of appendix B. The NACA uses a resistance-type thermometer having very low lag and a recovery factor of 0.99 ± 0.01. The inlet-duct method for measuring ram drag is probably the most accurate method, providing there is a suitable length of reasonably straight duct. Generally, total pressures are measured over equal area stations across the duct and are averaged by connecting to a single recorder. Measurement of static pressure at the duct walls has proved satisfactory and eliminates the hazard of flimsy stream static probes ahead of the engine. The method also eliminates the need for temperature measurements.

It has been suggested, at times, that the thrust of a turbojet engine be determined by measuring the forces on the engine mounts. Forces on the inlet cowling, inlet ducts, and tailpipe nozzle become appreciable and eliminate this possibility. A detailed discussion of these effects is given in reference 15.

Rocket engines.- The equations for computing the thrust of rocket engines are also presented in appendix B. Unlike the thrust of a turbojet engine, the thrust of a rocket engine can be determined by measuring the forces at the engine mounts. However, the method is infrequently used because the pressure method is simple and reliable and because it would be difficult to compensate for the Bourdon, and other adverse effects, of the large propellant lines attached to the engine. In using equation (B24), the thrust and exit areas are measured when the engine is cold; then, in order to compensate for changes that might occur when the engine is running, the nozzle coefficient C_f is determined by means of a thrust stand run. Nozzle coefficients determined in this manner are generally from 2 to 4 percent lower than the theoretical values determined from equation (B25).

Rocket engines designed for high altitude will overexpand the gases when on the ground so that the exit pressure p_e is less than atmospheric pressure p_0. There is evidence (ref. 16) that when the ratio of p_e/p_0 becomes 1/3 or smaller, the exhaust gases will separate from the nozzle walls and the area A_e becomes uncertain. There will also be a change in the nozzle coefficient C_f.

Static Pressure

Measurements of true static pressures are essential for the evaluation of dynamic pressure, Mach number, and engine thrust. Test aircraft at the NACA High-Speed Flight Station have the pitot-static head mounted on a boom extending ahead of the fuselage, as shown in figure 3. This installation positions the head as far ahead of the airplane as is practicable in order to minimize the influence of the airplane flow field at the pressure-sensing station. The total-pressure opening at the tip is the A-6 type of reference 17. The total-pressure readings are accurate within 1 percent for angles of attack from -20° to 40°; therefore, no corrections are needed. The static-pressure orifices are located along the top and bottom of the tube about 8 inches back of the tip in a manner that will minimize the effect of angle of attack. Static pressures measured from the orifices are subject to position errors at subsonic speeds. The position errors are largely a function of airplane configuration and the distance of the static-pressure orifices from the airplane; therefore, each installation is calibrated. Various methods for conducting calibrations of this nature have been suggested and used. These include the

radar-phototheodolite method (ref. 18), the accelerometer method (ref. 19), the temperature method (ref. 20), the radio altimeter method (ref. 21), and the more common tower-pass and pacer methods. The High-Speed Flight Station uses a modified radar-phototheodolite method almost exclusively, although the tower-pass and pacer methods have been used considerably in the past. The tower-pass method is considered the best from the standpoint of accuracy, but had to be abandoned because of the hazard of making very high-speed passes near the ground.

The radar-phototheodolite method has the advantage of providing static-pressure calibration data during routine research flights. The only additional equipment required in the test airplane is a radar beacon to aid in the tracking and to provide a means of synchronizing the radar-phototheodolite records with the airplane's internal records. With this method the radar and phototheodolite are used to determine the range and elevation angle of the airplane from which the true geometric altitude can be determined. The variation of atmospheric pressure with geometric altitude is determined by means of a radiosonde balloon survey made at the time of the flight. The method described in reference 18 has been modified for use at the High-Speed Flight Station so that the balloon is no longer tracked by the radar. It has been found more accurate to compute the altitude pressure survey from the simultaneous radiosonde measurements of temperature and pressure than to determine the balloon altitude by radar.

A comparison of the airspeed calibrations of 17 airplanes shows that the amount of error in Mach number due to position error in static-pressure measurements can be related to certain physical measurements on the airplane. Figure 9 shows the error in Mach number due to static-pressure error plotted against the ratio of boom length to the maximum effective fuselage diameter for subsonic, transonic, and supersonic speeds. Figure 10 shows the variations in Mach number error with Mach number for two airplanes having X/D ratios of 0.60 and 0.95, respectively. Above a Mach number of about 1.05, the corrections drop to zero or near zero.

Airplane Weight

Various methods are used to determine the airplane weight at any given instant during a flight. The most desirable system is some type of integrating flow meter inserted in the fuel line. Such flow meters can be of a recording type but frequently are merely visual meters in the cockpit. With visual meters, the pilot radios the reading to the ground at intervals so that a plot of airplane weight against flight time can be made and correlated with the various maneuvers. Less desirable, but still adequate, are nonintegrating recording fuel-rate meters which require a laborious integration during the reduction of the data. Fuel-tank-level meters are generally marginal in their accuracy, particularly where the readings vary with airplane attitude.

Rocket-propelled airplanes have high rates of fuel flow and large overall changes in weight because of fuel consumption; consequently, fuel flow must be determined with a higher percentage of accuracy. Suitable flow meters are available and have been used in at least one instance. With airplanes such as the X-1, where the thrust is varied only in fixed steps, the fuel consumption is directly proportional to the number of combustion chambers being operated, and the weight can be computed from the records of engine running time.

Control-Surface Position

In the performance of flight maneuvers to obtain drag data, it is necessary to vary the position of the longitudinal control surfaces to achieve the desired angle-of-attack variation. The control-surface positions have an effect on the drag results, and if comparisons of the data are to be made with other airplanes or wind-tunnel models they must be made under identical trim conditions. Consequently, the control-surface positions are measured during each flight maneuver. Trim effects are usually very large for tailless airplanes, but may become negligibly small on airplanes with small tail surfaces placed relatively far back of the wing. The measurements of directional and lateral control positions are used only for inspection and selection of comparable flight data.

Instruments for sensing the positions of the control surfaces are mounted at the surfaces in order to eliminate the effect of control-system deformations. This is particularly necessary for obtaining data at high indicated airspeeds. The spanwise location selected for the sensing elements is usually such as to give an approximate average surface deflection.

TREATMENT OF FLIGHT DATA

The total airplane drag at a given Mach number as determined by flight measurements is generally presented in the form of drag polars, which are plots of drag coefficient against lift coefficient. Each polar will represent a summation of drag components. At subsonic speeds these components will be the skin-friction drag and pressure drag, which together are referred to as the parasite drag; the induced drag, which is the drag associated with lift; and the trim drag, which is the drag associated with control-surface deflections. At supersonic speeds there will also be wave drag. It is sometimes desirable to separate the flight-determined drag data into its components; this can be accomplished with certain limitations.

The evaluation of trim drag may be arrived at by two methods. One method is to use wind-tunnel drag polars for a series of fixed positions

of the longitudinal control surfaces; the other method is to take flight measurements over a range of center-of-gravity positions. The magnitude and, hence, the importance of the trim drag will depend on the speed, static margin, and airplane configuration.

Other drag components can be derived by plotting the polar in the form of drag coefficient against the square of the lift coefficient. Figure 11 shows a typical plot of this type for the X-5 airplane. The linear portion of the curve is the true parabolic variation of the basic drag polar, and the slope of the line is a measure of the induced drag providing the data have been previously corrected for trim effects. The extension of the linear portion of the curve to zero lift is a measure of skin-friction drag and the actual value of drag at zero lift is a measure of the parasite drag.

COMPARISON OF FLIGHT AND WIND-TUNNEL DATA

Flight-test data and wind-tunnel-model data generally will not be in exact agreement and any meaningful comparison must be made on a component basis. Theoretically, there should be a decrease in skin-friction drag with increasing Reynolds number as indicated in figure 12 (ref. 22). The approximate Reynolds number regions for flight and wind-tunnel testing are indicated on this figure. Also shown are representative levels of zero-lift drag which represent the combination of friction and pressure drags.

It should be pointed out that additional differences between the flight and wind-tunnel data can be caused by deviation of the model from true scale, by lack of simulation of internal flows, by imperfect compensation for model support effects, and by differences in flow conditions such as transition points. If proper consideration is given to the above items, and if the trim conditions are identical, the flight and wind-tunnel data should be comparable.

CONCLUDING REMARKS

Experience in the flight measurement of drag on high-speed research airplanes and current fighter-type airplanes at the NACA High-Speed Flight Station has shown that the accelerometer method is the most satisfactory method for determining the total airplane drag in flight research. The accurate measurement of longitudinal acceleration required by the accelerometer method can be made by means of specially constructed mechanical accelerometers.

The use of a pitot-static head and angle-of-attack vane system mounted forward of the fuselage produces accurate measurements at supersonic speeds. Adequate techniques are available to determine the errors at subsonic speeds.

Satisfactory methods for determining in flight the thrust of turbojet-afterburner and rocket engines have been developed. Present developments in the techniques indicate that the methods can be adapted satisfactorily to advanced engines having variable-geometry inlet and exit ducts.

In order to assess the reliability of comparisons of wind-tunnel and flight measurements of airplane drag, it is important to know the actual model configuration and the flow conditions under which the wind-tunnel investigation was conducted.

High-Speed Flight Station,
National Advisory Committee for Aeronautics,
Edwards, Calif., July 19, 1956.

APPENDIX A

DERIVATION OF DRAG EQUATIONS

In an evaluation of the drag of an airplane, reference is made to the forces and angles shown in the following sketch:

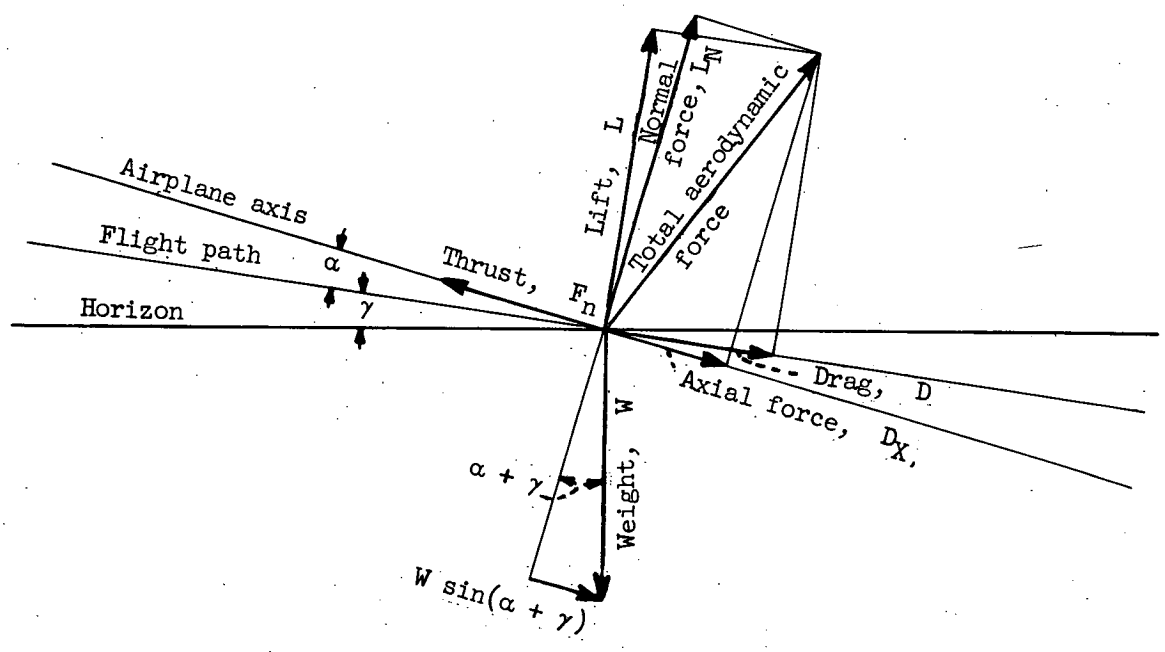

The equations used for drag reduction by the accelerometer and energy methods are derived in the following sections.

Accelerometer Method

Taking a summation of the forces along the airplane axis and equating them to zero yields

$$F_n - D_X - W \sin(\alpha + \gamma) - WA_X = 0 \qquad (A1)$$

Because the longitudinal accelerometer is also affected by gravity,

$$A_X = A_L - \sin(\alpha + \gamma) \qquad (A2)$$

Combining equations (A1) and (A2) gives

$$F_n - D_X - W \sin(\alpha + \gamma) - W\left[A_L - \sin(\alpha + \gamma)\right] = 0$$

$$F_n - D_X - WA_L = 0$$

$$D_X = F_n - WA_L \tag{A3}$$

Reducing equation (A3) to coefficient form yields

$$C_X = \frac{D_X}{qS} = \frac{F_n - WA_L}{qS} \tag{A4}$$

Taking a summation of the forces perpendicular to the airplane axis and equating them to zero gives

$$W \cos(\alpha + \gamma) - L_N + WA_Z = 0 \tag{A5}$$

Because the normal accelerometer is also affected by gravity,

$$A_Z = n - \cos(\alpha + \gamma) \tag{A6}$$

Combining equations (A5) and (A6),

$$W \cos(\alpha + \gamma) - L_N + Wn - W \cos(\alpha + \gamma) = 0$$

$$L_N = nW \tag{A7}$$

Reducing equation (A7) to coefficient form gives

$$C_N = \frac{L_N}{qS} = \frac{nW}{qS} \tag{A8}$$

The force coefficients of equations (A4) and (A8) can be converted from the airplane axis to the flight-path axis as follows:

$$C_D = C_X \cos \alpha + C_N \sin \alpha \tag{A9}$$

$$C_L = C_N \cos \alpha - C_X \sin \alpha \tag{A10}$$

Energy Method

The total airplane energy may be expressed as

$$E_A = Wh + \frac{WV_0^2}{2g} \tag{A11}$$

If airplane weight is assumed to be constant over the incremental time period,

$$\frac{dE_A}{dt} = W\left(\frac{dh}{dt} + \frac{1}{g} V_0 \frac{dV_0}{dt}\right) \tag{A12}$$

Only the thrust and drag forces contribute to the energy change

$$\frac{dE_A}{dt} = \left(F_n \cos \alpha - D\right)V_0 \tag{A13}$$

Combining equations (A12) and (A13) gives

$$\left(F_n \cos \alpha - D\right)V_0 = W\left(\frac{dh}{dt} + \frac{1}{g} V_0 \frac{dV_0}{dt}\right)$$

and

$$D = F_n \cos \alpha - W\left(\frac{\frac{dh}{dt}}{V_0} + \frac{\frac{dV_0}{dt}}{g}\right)$$

or, in coefficient form,

$$C_D = \frac{F_n \cos \alpha}{qS} - \frac{W}{qS}\left(\frac{\frac{dh}{dt}}{V_0} + \frac{\frac{dV_0}{dt}}{g}\right) \tag{A14}$$

Because altitudes are determined from pressure measurements, it is desirable to convert dh/dt as follows:

$$\frac{dh}{dt} = \frac{dp_0}{dt}\frac{dh}{dp_0} = \frac{dp_0}{dt}\frac{1}{\rho_0}$$

Then,

$$C_D = \frac{F_n \cos \alpha}{qS} - \frac{W}{qS}\left(\frac{\frac{dp_0}{dt}}{\rho_0 V_0} + \frac{\frac{dV_0}{dt}}{g}\right) \tag{A15}$$

APPENDIX B

DERIVATION OF THRUST EQUATIONS

Turbojet Engine (Including Afterburner)

Jet thrust.- The compressible-flow relationship for a fluid flowing from point 1 to point 2 can be derived from the following three relationships:

Energy (Bernoulli's equation):

$$\int_{V_1}^{V_2} V\,dV + \int_{p_1}^{p_2} \frac{dp}{\rho} = 0 \tag{B1}$$

Adiabatic compression:

$$\frac{p}{\rho^{\gamma}} = c \tag{B2}$$

Continuity:

$$w = \rho A V \tag{B3}$$

Rearranging equation (B2), substituting into equation (B1), and integrating gives

$$\frac{1}{\rho} = c'(p)^{-\frac{1}{\gamma}}$$

$$\int_{V_1}^{V_2} V\,dV + \int_{p_1}^{p_2} c'(p)^{-\frac{1}{\gamma}}\,dp = 0$$

$$\frac{V_2^2 - V_1^2}{2} + c'\,\frac{\gamma}{\gamma - 1}\left(p_2^{\frac{\gamma-1}{\gamma}} - p_1^{\frac{\gamma-1}{\gamma}}\right) = 0 \tag{B4}$$

Let

$$V_1 = 0$$

Then

$$p_1 = P_1$$

For the adiabatic condition, $P_1 = P_2$; hence $p_1 = P_2$ and

$$\frac{V_2^2}{2} = -c' \frac{\gamma}{\gamma - 1}\left(p_2^{\frac{\gamma-1}{\gamma}} - P_2^{\frac{\gamma-1}{\gamma}}\right)$$

The equation is now applicable to a single point (2), and hence, is applicable to all points:

$$V = \sqrt{2c' \frac{\gamma}{\gamma - 1}\left(P^{\frac{\gamma-1}{\gamma}} - p^{\frac{\gamma-1}{\gamma}}\right)} \tag{B5}$$

where

$$c' = \frac{p^{1/\gamma}}{\rho}$$

If a perfect gas is assumed,

$$\rho = \frac{p}{RT} \tag{B6}$$

Then

$$c' = p^{1/\gamma} \frac{RT}{p} = \frac{RT}{p^{\frac{\gamma-1}{\gamma}}}$$

and

$$V = \sqrt{2 \frac{RT}{p^{\frac{\gamma-1}{\gamma}}} \frac{\gamma}{\gamma - 1}\left(P^{\frac{\gamma-1}{\gamma}} - p^{\frac{\gamma-1}{\gamma}}\right)}$$

$$= \sqrt{RT \frac{2\gamma}{\gamma - 1}\left[\left(\frac{P}{p}\right)^{\frac{\gamma-1}{\gamma}} - 1\right]} \tag{B7}$$

Since momentum $= wV = \rho AV^2$,

$$wV = \rho A\, RT \frac{2\gamma}{\gamma - 1}\left[\left(\frac{P}{p}\right)^{\frac{\gamma-1}{\gamma}} - 1\right] \tag{B8}$$

By use of equation (B6) to eliminate ρ,

$$wV = Ap \frac{2\gamma}{\gamma - 1}\left[\left(\frac{P}{p}\right)^{\frac{\gamma-1}{\gamma}} - 1\right] \tag{B9}$$

If p is not equal to ambient pressure, then a pressure term must be added to obtain the jet thrust

$$F_j = wV + A(p - p_0)$$

$$F_j = Ap \frac{2\gamma}{\gamma - 1}\left[\left(\frac{P}{p}\right)^{\frac{\gamma-1}{\gamma}} - 1\right] + A(p - p_0) \tag{B10}$$

When the tailpipe pressure ratio is subcritical $\left[\frac{P}{p_0} < \left(\frac{\gamma + 1}{2}\right)^{\frac{\gamma}{\gamma-1}}\right]$, the flow is subsonic and p is assumed equal to p_0; the jet thrust is thus exactly equal to the momentum force. Equation (B10) then becomes

$$F_j = Ap_0 \frac{2\gamma}{\gamma - 1}\left[\left(\frac{P}{p_0}\right)^{\frac{\gamma-1}{\gamma}} - 1\right] \tag{B11}$$

For sonic tailpipe velocities $\left[\frac{P}{p_0} \geq \left(\frac{\gamma + 1}{2}\right)^{\frac{\gamma}{\gamma-1}}\right]$, it is sometimes assumed that

$$p = \frac{P}{\left(\frac{\gamma + 1}{2}\right)^{\frac{\gamma}{\gamma-1}}}$$

and equation (B10) reduces to

$$F_j = A\left[(\gamma + 1)p - p_0\right]$$

or

$$F_j = A\left[\left(\frac{2}{\gamma + 1}\right)^{\frac{\gamma}{\gamma-1}}(\gamma + 1)P - p_0\right] \tag{B12}$$

For nonafterburner operation, γ is generally assumed to be 1.33 and equation (B12) becomes

$$F_j = A(1.259P - p_0) \tag{B13}$$

For afterburner operation γ is generally assumed to be 1.25, and equation (B12) becomes

$$F_j = A(1.249P - p_0) \tag{B14}$$

The values of jet thrust as given by equations (B11) to (B14) are theoretical and, in order to account for deviation from perfect gas conditions and other assumptions, as well as to compensate for some of the inadequacies of the instrumentation, the jet thrust is multiplied by a nozzle coefficient C_f which is determined by experiment as a function of pressure ratio P/p_0.

Ram drag.- The equations used to determine ram drag are:

$$F_r = \text{Momentum of inlet air} = \frac{V_0 w_a}{g}$$

$$V_0 = Ma_0 = M\sqrt{\gamma g R T_0}$$

$$F_r = \frac{w_a M}{g}\sqrt{\gamma g R T_0} \tag{B15}$$

Three methods are commonly employed for determining the air flow through the engine:

(1) Tailpipe-temperature method. In this method equations (B3), (B6), and (B7) are combined

$$w = \rho A\sqrt{RT\,\frac{2\gamma}{\gamma - 1}\left[\left(\frac{P}{p}\right)^{\frac{\gamma-1}{\gamma}} - 1\right]}$$

$$w = \frac{pA}{RT}\sqrt{RT\,\frac{2\gamma}{\gamma - 1}\left[\left(\frac{P}{p}\right)^{\frac{\gamma-1}{\gamma}} - 1\right]}$$

$$w = \frac{Ap}{\sqrt{RT}}\sqrt{\frac{2\gamma}{\gamma - 1}\left[\left(\frac{P}{p}\right)^{\frac{\gamma-1}{\gamma}} - 1\right]} \tag{B16}$$

The gas flow at the tailpipe includes both air and fuel, so that, for tailpipe measurements,

$$w_a = \frac{Ap}{\sqrt{RT}}\sqrt{\frac{2\gamma}{\gamma - 1}\left[\left(\frac{P}{p}\right)^{\frac{\gamma-1}{\gamma}} - 1\right]} - w_f \tag{B17}$$

(2) Engine-compressor method. Most turbojet engines have compressors that can be assumed to be a constant-volume pump and the manufacturer's plots of $\frac{w_a\sqrt{\theta}}{g}$ plotted against $\frac{N}{\sqrt{\theta}}$ are generally applicable to all engines of a type. The quantity θ is the total temperature of the air entering the compressor divided by sea-level standard temperature (518.4° R), and the quantity δ is the total pressure of the air entering the compressor divided by sea-level standard pressure (2116 lb/sq ft).

(3) Inlet-duct method. If the inlet duct has a straight section of reasonable length, the air flow can be determined from static- and total-pressure surveys across the duct:

$$\begin{aligned} w_a &= \rho_d A_d V_d \\ &= \rho_d A_d M_d a_d \\ &= \rho_d A_d M_d \sqrt{\gamma g R T_d} \end{aligned} \tag{B18}$$

Combining equations (B6) and (B18) gives

$$\begin{aligned} w_a &= \frac{p_d}{RT_d} A_d M_d \sqrt{\gamma g R T_d} \\ &= p_d A_d M_d \sqrt{\frac{\gamma g}{R T_d}} \end{aligned} \tag{B19}$$

If equations (B15) and (B19) are combined,

$$F_r = \frac{M}{g}\sqrt{\gamma g R T_0}\; p_d A_d M_d \sqrt{\frac{\gamma g}{R T_d}} \tag{B20}$$

The total temperature of the air can be assumed constant up to the compressor face

$$\begin{aligned} T_t &= T_0\left(1 + \frac{\gamma - 1}{2} M^2\right) \\ &= T_d\left(1 + \frac{\gamma - 1}{2} M_d^2\right) \end{aligned} \tag{B21}$$

For air, γ will have a value of 1.4, and equation (B21) becomes

$$\frac{T_0}{T_d} = \frac{1 + 0.2M_d^2}{1 + 0.2M^2} \tag{B22}$$

Combining equations (B20) and (B22) gives

$$F_r = p_d A_d M M_d \gamma \sqrt{\frac{1 + 0.2M_d^2}{1 + 0.2M^2}} \tag{B23}$$

Rocket-Engine Thrust

The thrust of a rocket engine can be derived from the fundamental flow equations in the same manner as equation (B10), and this equation is directly applicable to rocket engines. However, it is impractical to make measurements at the nozzle exit because of the high temperatures involved. The equation is therefore modified to the following, theoretical relationships being used:

$$F_n = A_t p_c C_f + A_e(p_e - p_0) \tag{B24}$$

where

$$C_f = \gamma \sqrt{\frac{2}{\gamma - 1}\left(\frac{2}{\gamma + 1}\right)^{\frac{\gamma+1}{\gamma-1}}\left[1 - \left(\frac{p_e}{p_c}\right)^{\frac{\gamma-1}{\gamma}}\right]} \tag{B25}$$

and p_e can be obtained from the relationship

$$\frac{A_t}{A_e} = \left(\frac{\gamma + 1}{2}\right)^{\frac{1}{\gamma-1}}\left(\frac{p_e}{p_c}\right)^{\frac{1}{\gamma}} \sqrt{\left(\frac{\gamma + 1}{\gamma - 1}\right)\left[1 - \left(\frac{p_e}{p_c}\right)^{\frac{\gamma-1}{\gamma}}\right]} \tag{B26}$$

The complete derivation of equations (B24), (B25), and (B26) is given in reference 23.

REFERENCES

1. Smith, F., and Thom, A. W.: Note on the Use of a Longitudinal Accelerometer for Measuring Aircraft Drag in Flight in the Dive. TN No. Aero. 1649, British R.A.E., 1945.

2. Keller, Thomas L., and Keuper, Robert F.: Comparison of the Energy Method With the Accelerometer Method of Computing Drag Coefficients From Flight Data. NACA WR A-57, 1945. (Formerly NACA CB 5H31.)

3. Pearson, Henry A., and Beadle, Dorothy E.: Flight Measurements by Various Methods of the Drag Characteristics of the XP-51 Airplane. NACA WR L-741, 1946. (Formerly NACA MR L6F12.)

4. Harrington, Russel M., and Shoemacher, Paul E.: Flight Test Engineering Manual, USAF Tech. Rep. No. 6273, revised Jan. 1953. USAF, ARDC, AFFTC, EAFB, Edwards, Calif., section 4, pp. 42-43.

5. Allen, H. Julian, and Perkins, Edward W.: A Study of Effects of Viscosity on Flow Over Slender Inclined Bodies of Revolution. NACA Rep. 1048, 1951. (Supersedes NACA TN 2044.)

6. Pearson, Albin O., and Brown, Harold A.: Calibration of a Combined Pitot-Static Tube and Vane-Type Flow Angularity Indicator at Transonic Speeds and at Large Angles of Attack or Yaw. NACA RM L52F24, 1952.

7. Sinclair, Archibald R., and Mace, William D.: Wind-Tunnel Calibration of a Combined Pitot-Static Tube and Vane-Type Flow-Angularity Indicator at Mach Numbers of 1.61 and 2.01. NACA TN 3808, 1956.

8. Glauert, H.: The Elements of Aerofoil and Airscrew Theory. Second ed., Cambridge Univ. Press, 1947. (Reprinted 1948.)

9. Yaggy, Paul F.: A Method for Predicting the Upwash Angles Induced at the Propeller Plane of a Combination of Bodies With an Unswept Wing. NACA TN 2528, 1951.

10. Rogallo, Vernon L.: Effects of Wing Sweep on the Upwash at the Propeller Planes of Multiengine Airplanes. NACA TN 2795, 1952.

11. Rolls, L. Stewart, Havill, C. Dewey, and Holden, George R.: Techniques for Determining Thrust in Flight for Airplanes Equipped With Afterburners. NACA RM A52K12, 1953.

12. Stephenson, J., Shields, R. T., and Bottle, D. W.: An Investigation into the Pitot Rake Method of Measuring Turbo Jet Engine Thrust in Flight. C.P. No. 143, British A.R.C., 1954.

13. Walchner, O.: The Effect of Compressibility on the Pressure Reading of a Prandtl Pitot Tube at Subsonic Flow Velocity. NACA TM 917, 1939.

14. Krause, Lloyd N.: Effects of Pressure-Rake Design Parameters on Static-Pressure Measurement for Rakes Used in Subsonic Free Jets. NACA TN 2520, 1951.

15. Jakobsson, Bengt: Definition and Measurement of Jet Engine Thrust. Jour. R.A.S., vol. LV, Apr. 1951, pp. 226-243.

16. Durham, Franklin P., and Wood, K. D.: The Performance Characteristics of Small Rocket-Type Nozzles. Part II. Rep. 3 (Contract No. N-123S-82337), Eng. Exp. Station, Univ. of Colorado, Sept. 1953.

17. Gracey, William, Letko, William, and Russell, Walter R.: Wind-Tunnel Investigation of a Number of Total-Pressure Tubes at High Angles of Attack - Subsonic Speeds. NACA TN 2331, 1951. (Supersedes NACA RM L50G19.)

18. Zalovcik, John A.: A Radar Method of Calibrating Airspeed Installations on Airplanes in Maneuvers at High Altitudes and at Transonic and Supersonic Speeds. NACA Rep. 985, 1950. (Supersedes NACA TN 1979.)

19. Zalovcik, John A., Lina, Lindsay J., and Trant, James P., Jr.: A Method of Calibrating Airspeed Installations on Airplanes at Transonic and Supersonic Speeds by the Use of Accelerometer and Attitude-Angle Measurements. NACA Rep. 1145, 1953. (Supersedes NACA TN 2099 by Zalovcik and NACA TN 2570 by Lina and Trant.)

20. Zalovcik, John A.: A Method of Calibrating Airspeed Installations on Airplanes at Transonic and Supersonic Speeds by Use of Temperature Measurements. NACA TN 2046, 1950.

21. Thompson, Jim Rogers, and Kurbjun, Max C.: Evaluation of the Accuracy of an Aircraft Radio Altimeter for Use in a Method of Airspeed Calibration. NACA TN 3186, 1954.

22. Van Driest, E. R.: Turbulent Boundary Layer in Compressible Fluids. Jour. Aero. Sci., vol. 18, no. 3, Mar. 1951, pp. 145-160, 216.

23. Sutton, George P.: Rocket Propulsion Elements. John Wiley & Sons, Inc., 1949, ch. 3.

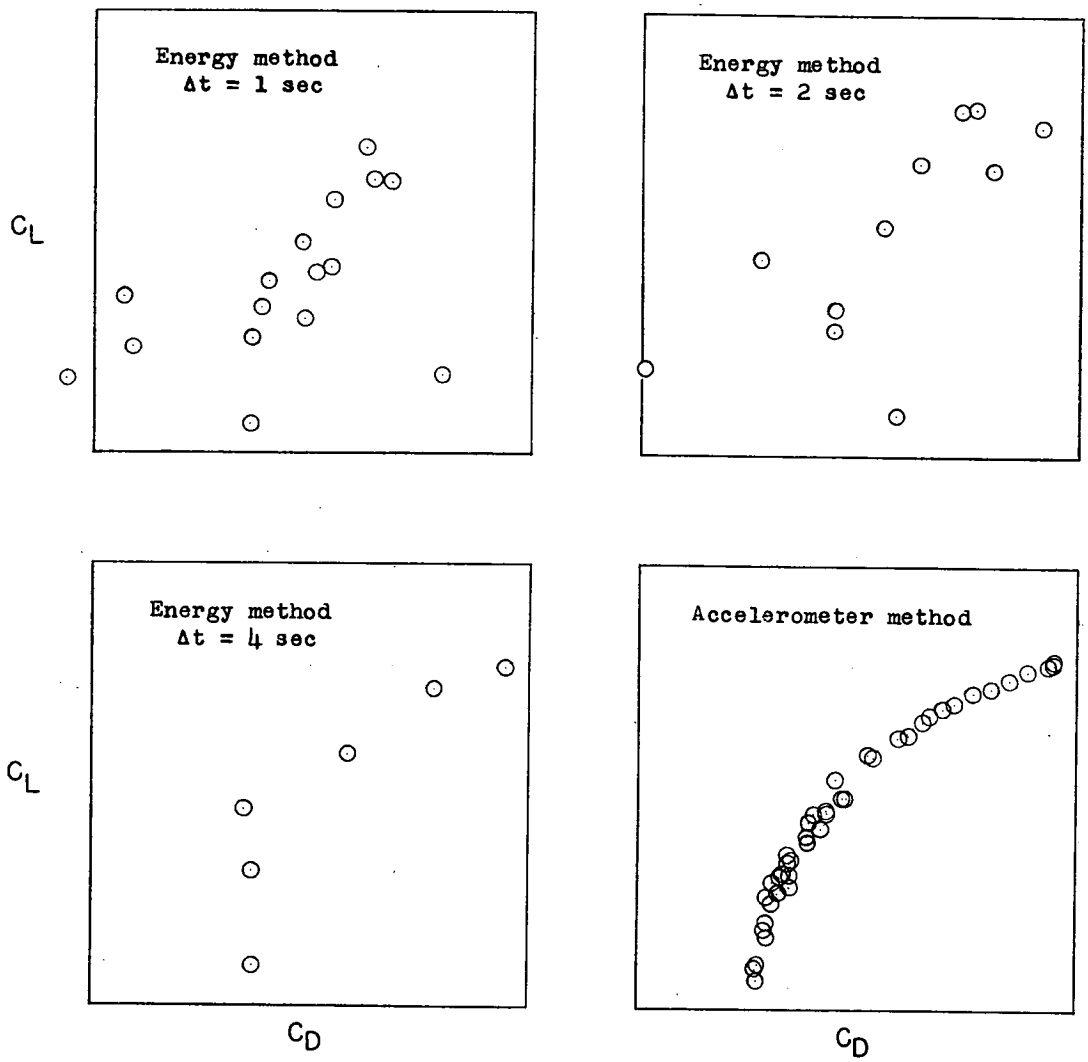

Figure 1.- Comparison of drag coefficients determined by energy and accelerometer methods for a typical push-down, pull-up maneuver.

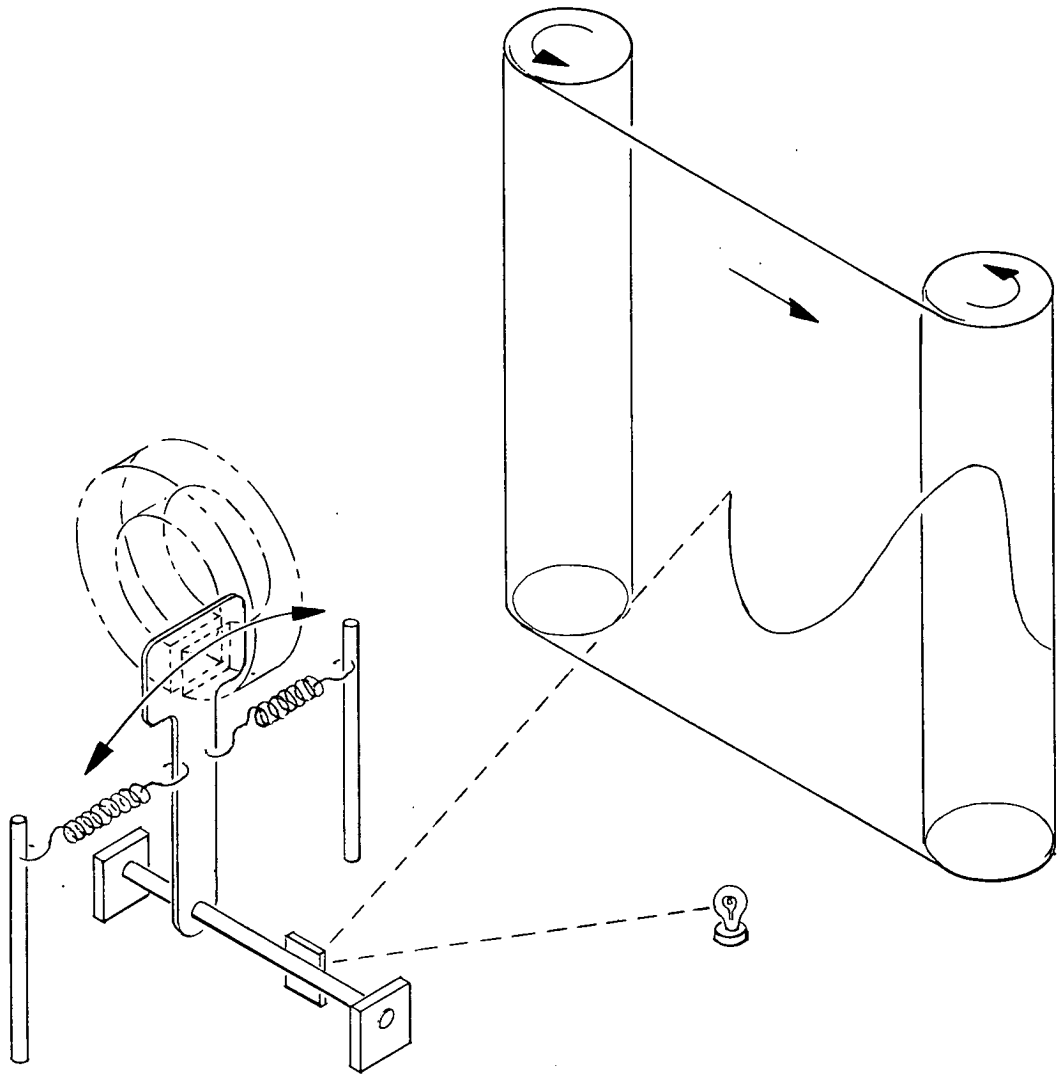

Figure 2.- Schematic diagram of NACA magnetically damped accelerometer.

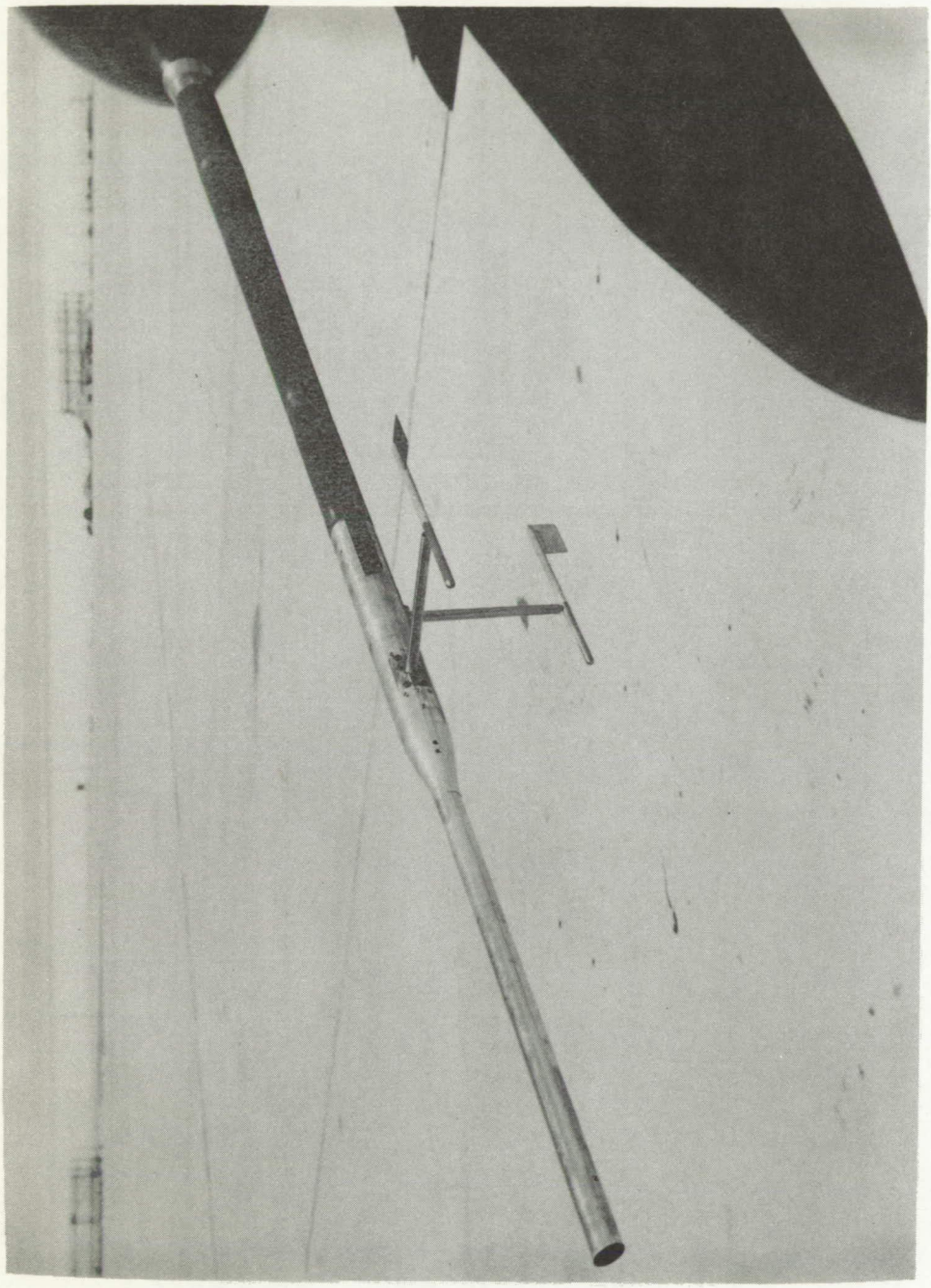

E-2357

Figure 3.- Typical fuselage nose-boom installation showing pitot-static head and angle-of-attack and angle-of-sideslip vanes.

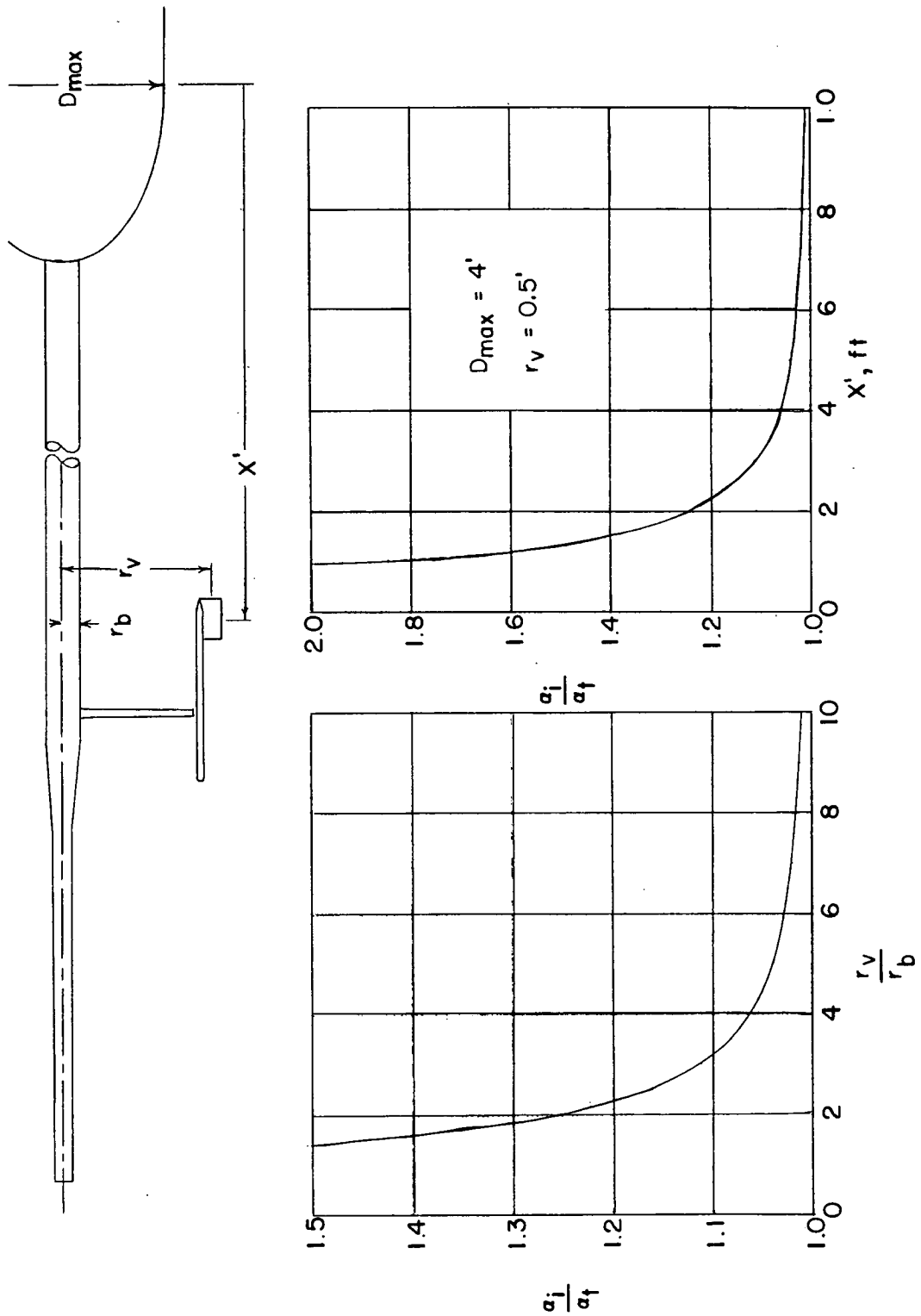

Figure 4.- Theoretical effects on angle-of-attack measurements of upwash from the nose boom and fuselage at low speeds.

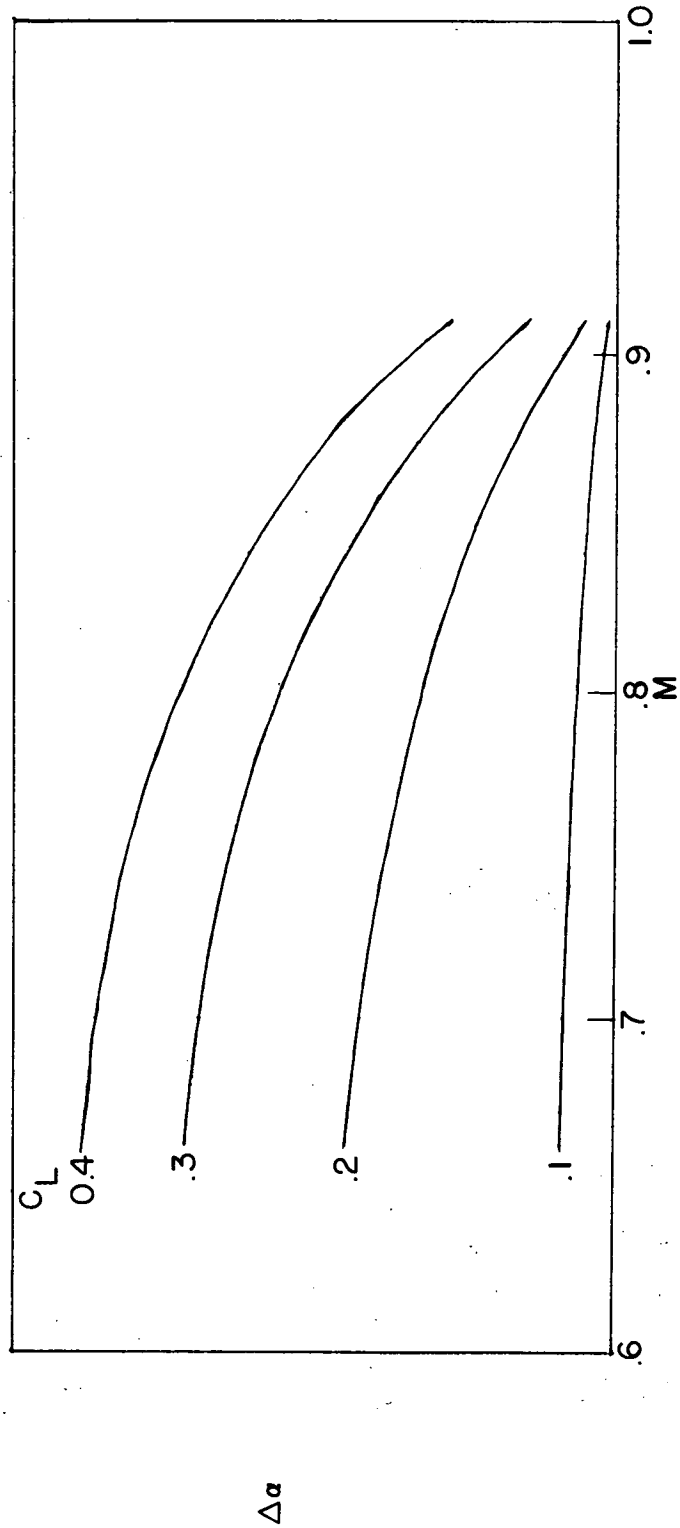

Figure 5.- The variation of angle-of-attack error due to upwash with Mach number and lift coefficient.

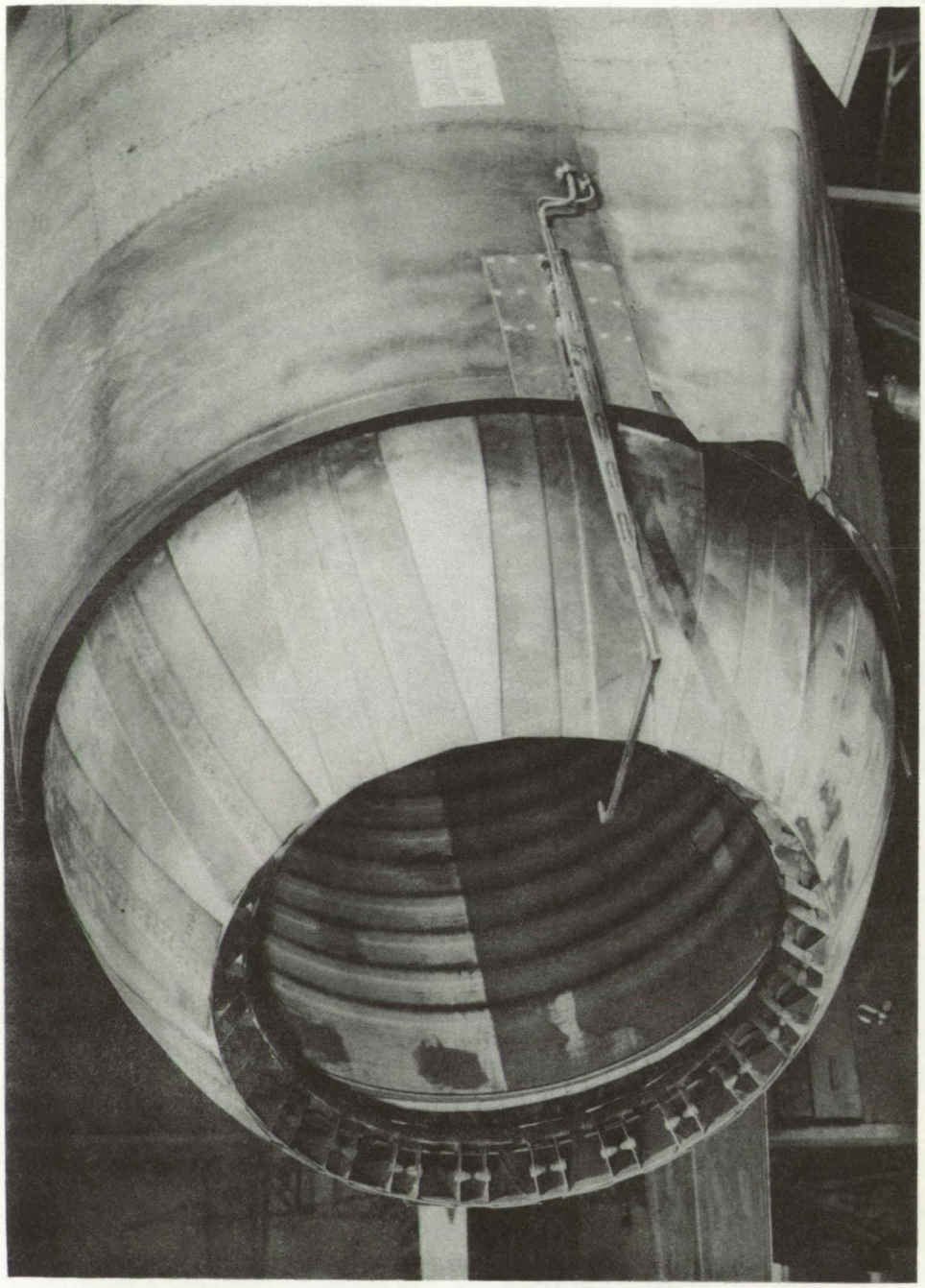

E-2065

Figure 6.- Air-cooled, fixed pitot probe for the measurement of jet thrust of turbojet engine-afterburner combination.

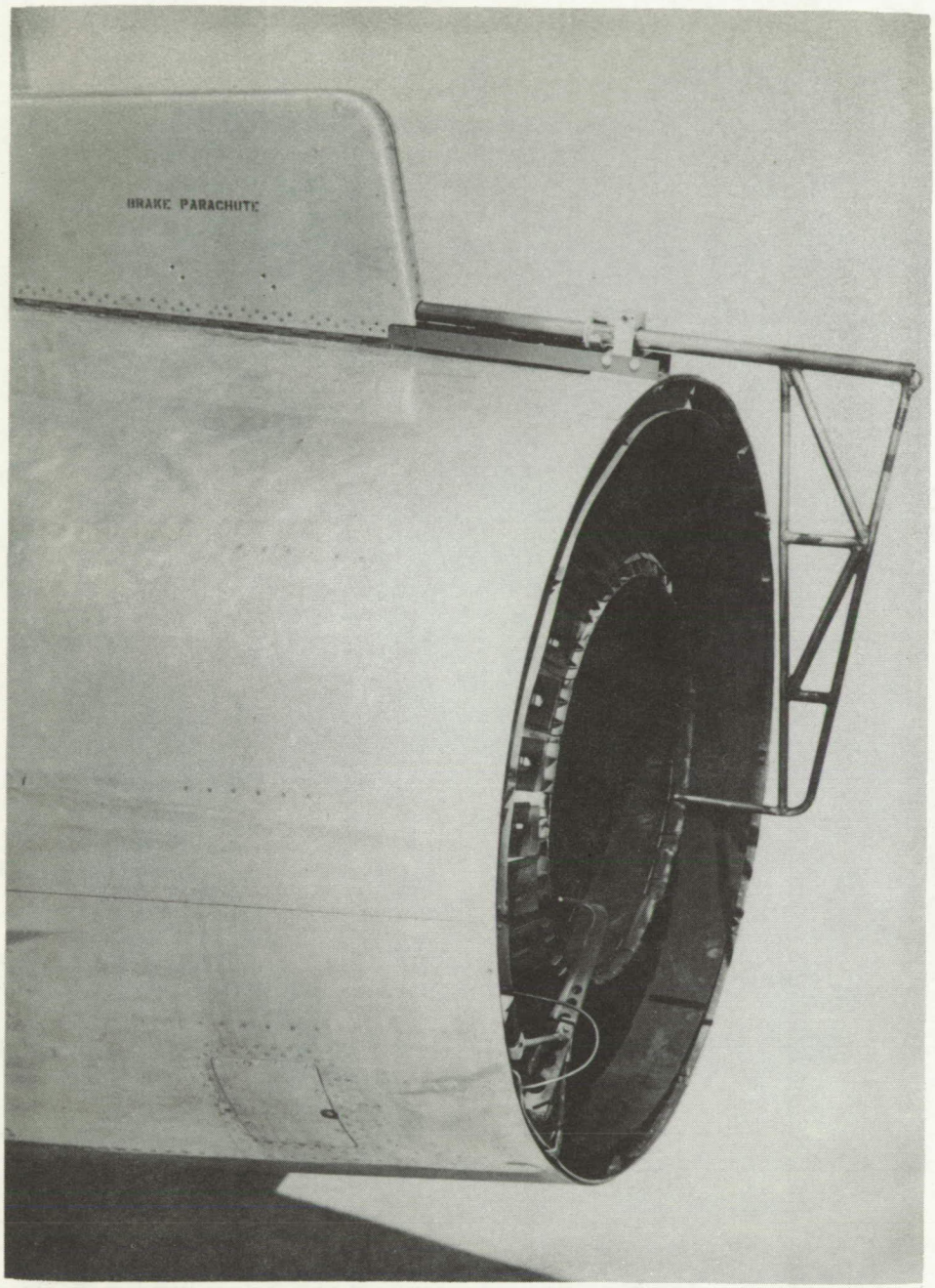

E-2375

Figure 7.- Swinging pitot probe for the measurement of total-pressure profiles across the exit of a turbojet engine-afterburner combination.

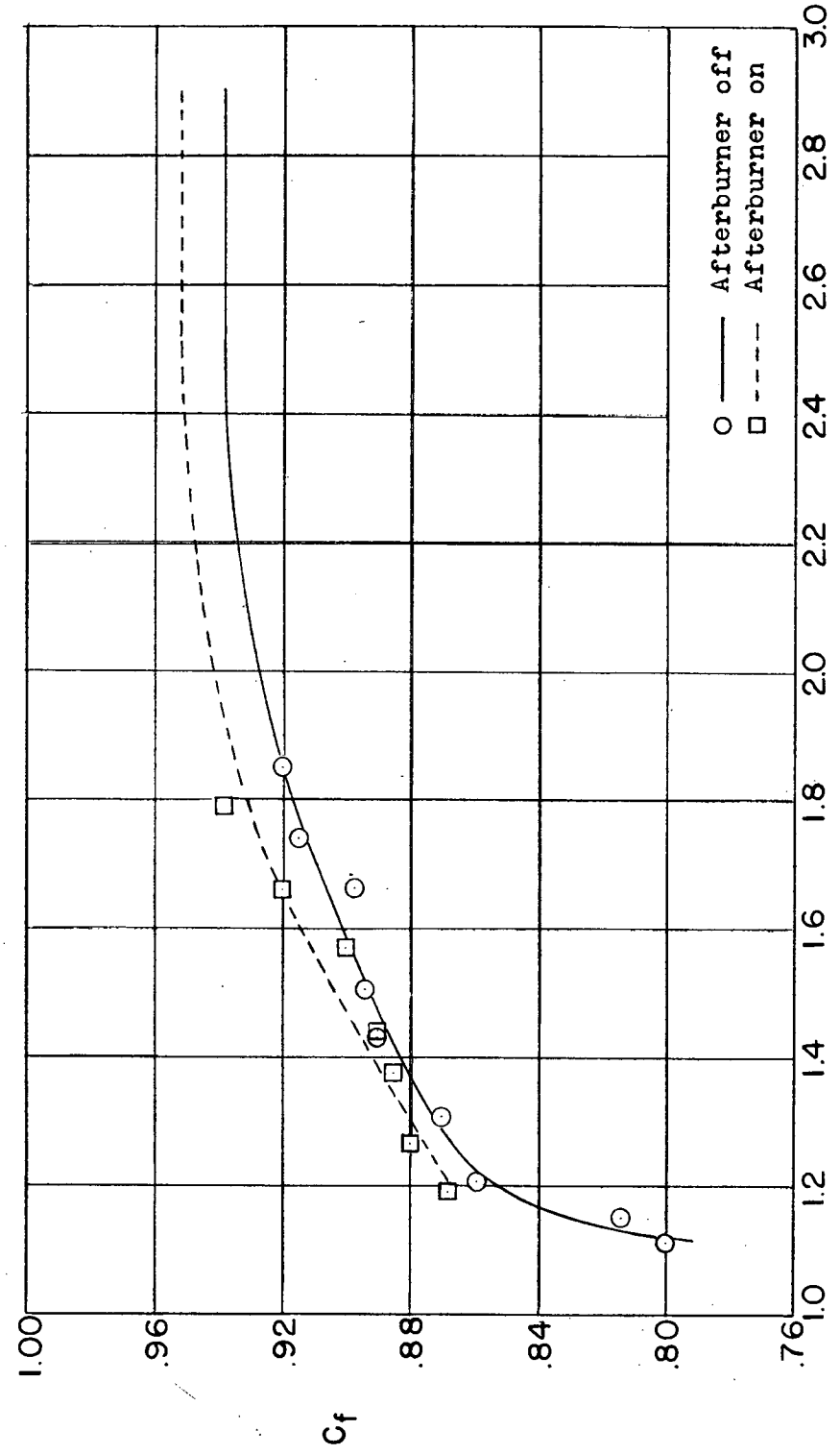

Figure 8.- Typical nozzle calibration for a turbojet engine.

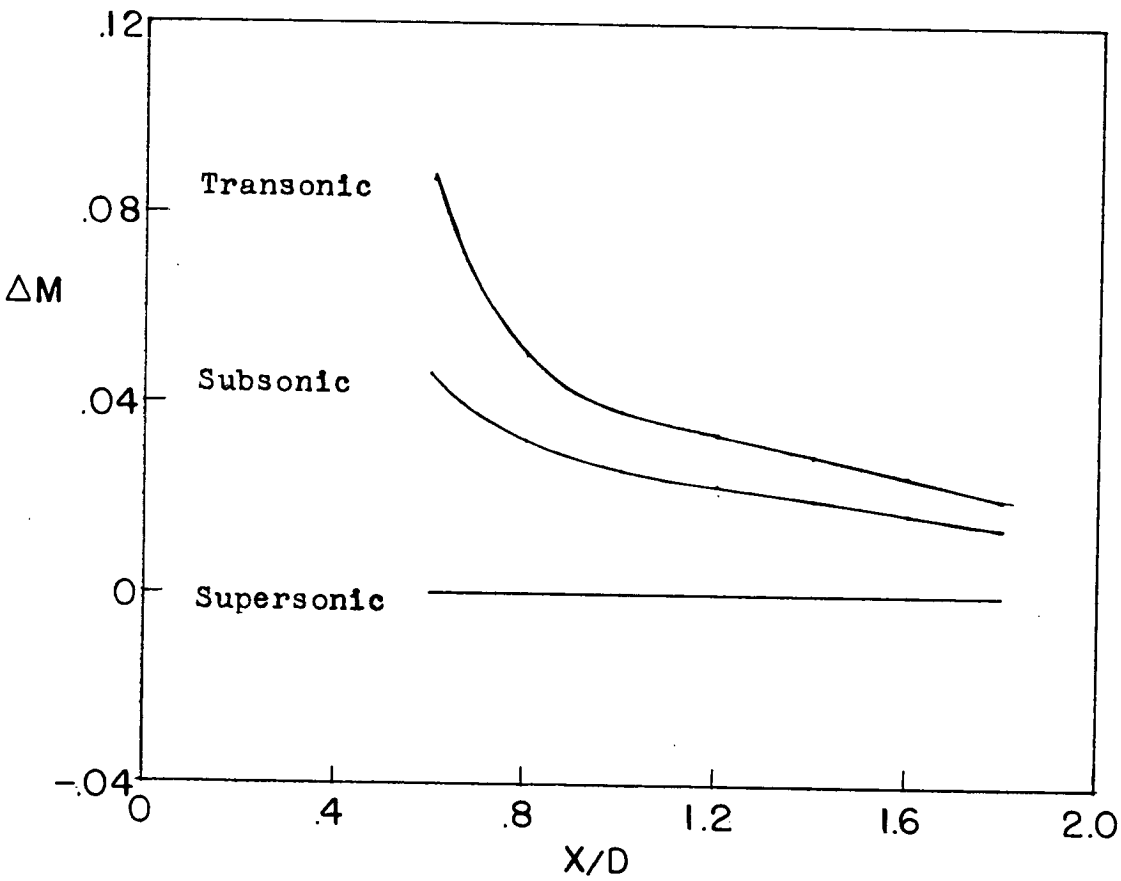

Figure 9.- Effect of ratio of boom length to fuselage diameter on Mach number error.

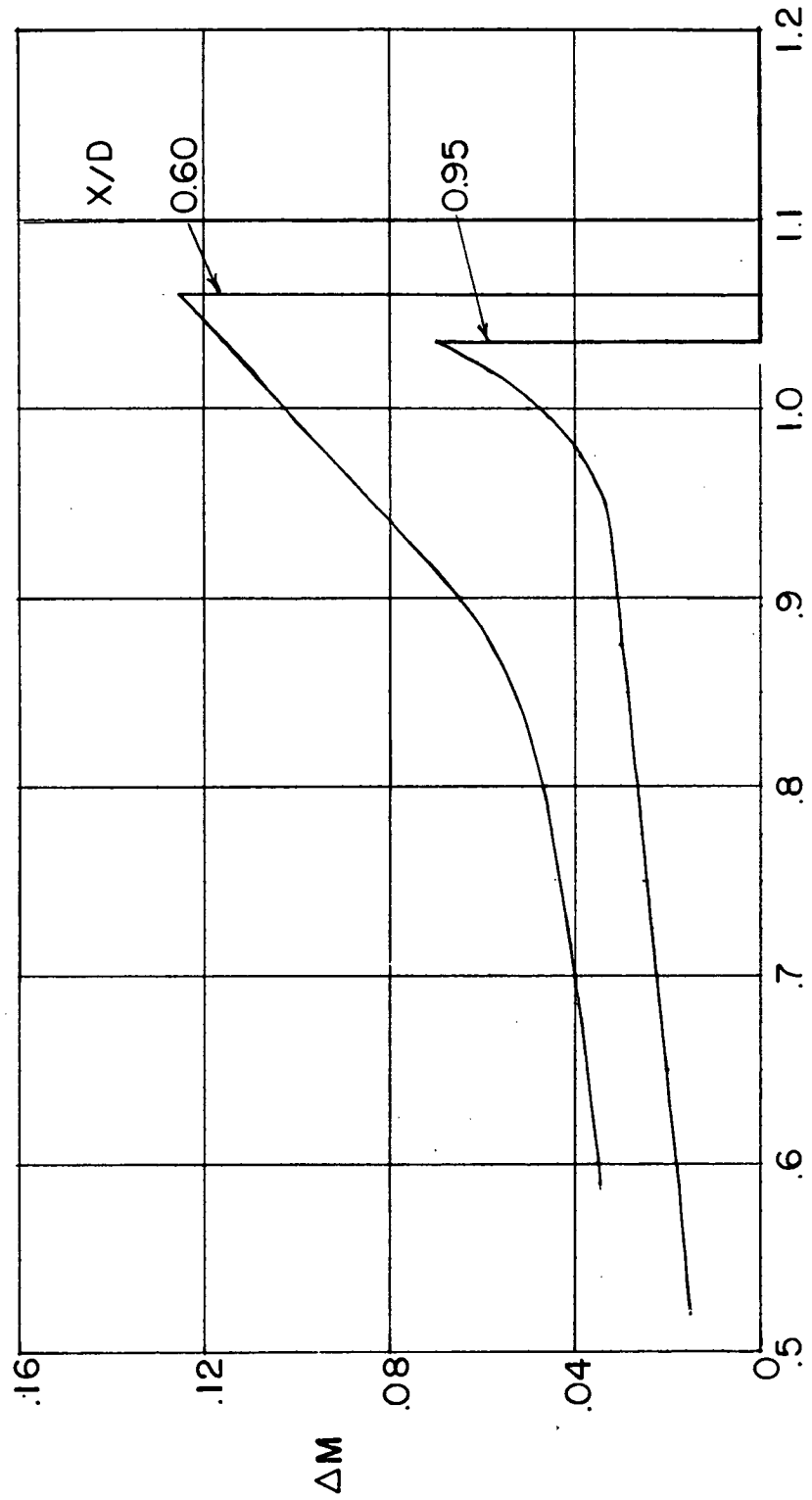

Figure 10.- Variation of Mach number error with Mach number.

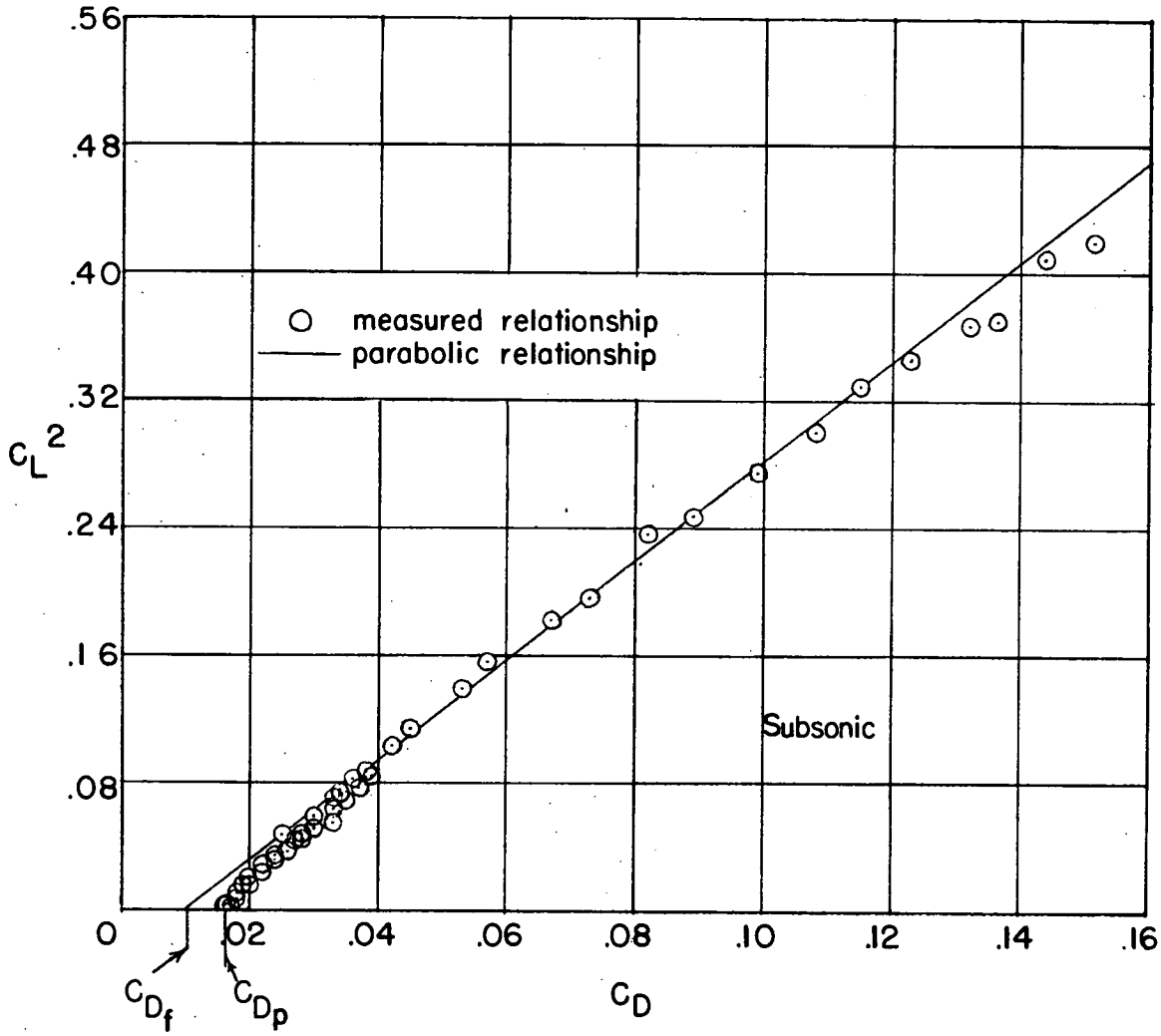

Figure 11.- Variation of C_D with C_L^2 showing deviation of data from theoretical parabolic relationship for 60° sweptback wing.

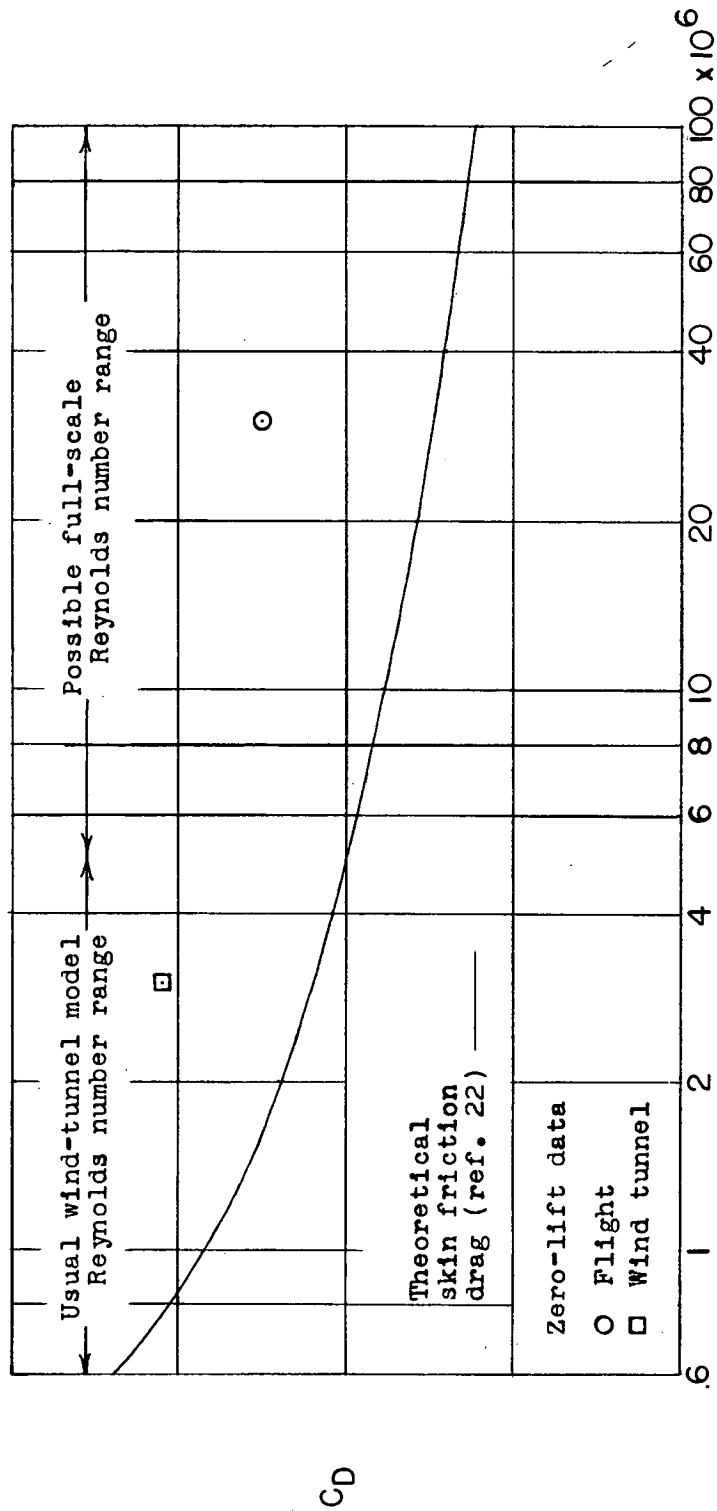

Figure 12.- Effect of Reynolds number on the theoretical skin-friction drag and on the comparison of flight and wind-tunnel zero-lift drag data.